A NEW ALGORITHM FOR NAVIGATION BY SKYLIGHT BASED ON INSECT VISION

F. J. Smith
School of Electronics, Electrical Engineering and Computer Science
Queens University, Belfast, N. Ireland

Keywords: Polarization, skylight, navigation, insect vision, POL, insect celestial map, robot, drone.

Abstract: Many insects can navigate accurately using the polarised light from the sky when the sun is obscured. They navigate using two different types of optical features: one is a set of three ocelli on the top of the head and the second is a celestial compass based on several photoreceptors on the dorsal rims of the compound eyes. Either feature can be used alone, but the dorsal rim receptors appear to be more accurate. Robots have been built that navigate using three photoreceptors, or three pairs of orthogonally oriented photoreceptors, but none has been designed which uses a full set of photoreceptors similar to those in the dorsal rim. A new model of the function of the dorsal rim compass is proposed which relies on the four azimuths at which the polarization angle $\chi = \pm\pi/4$. A simulation shows that this could provide an accurate navigational tool for a robot (or insect) in lightly clouded skies.

1 INTRODUCTION

Due to the scattering of light within the earth's atmosphere, skylight is partially linearly polarized, discovered by the Irish Scientist Tyndall (1869). Two years later a full mathematical description of the phenomenon was given by Lord Rayleigh (1871) for the scattering by small particles in the atmosphere (the particles we now know are air molecules). That an insect can use this polarization to navigate was first discovered in experiments with bees by Karl von Frisch (1949).

It took another 25 years before the nature of the insect's celestial compass began to be clarified (Kirshfeld et al., 1975; Bernard and Wehner, 1977). There are two different types of optical features involved: the first is a set of ocelli, generally 3 in number, on the top of the head (Goodman, 1970) and the second depends primarily on a specialized part of the insect compound eye, a comparatively small group of ommatidia situated in the dorsal rim area. Normally the ocelli and dorsal rim are probably used together to navigate, in some way still unknown, but experiments with desert ants (Fent and Wehner, 1985) have shown that either feature can be used successfully alone with the other blacked out. It was also found in these experiments that the ocelli are more erratic and less accurate for navigation than the dorsal rim photoreceptors.

Further insight on the dorsal rim came from Rudiger Wehner and co-workers working with desert ants and bees (Labhart, 1980; Rossel and Wehner, 1982; Wehner, 1997). It was found that each ommatidium in the dorsal rim has two photoreceptors with axes of polarization at right angles to one another and each strongly sensitive to the E-vector orientation of plane polarized light. One of the axes of polarization of these ommatidia has a fan shaped orientation that has been shown in experiments to provide a map for the polarised sky, a map which the insect can use as a compass (Rossel, 1993). Recently this insect map of celestial E-vector orientation has been found represented within the central complex of the brain of an insect, the cricket (Heinz and Homberg, 2007). We return to this later.

Therefore much is known about this celestial compass and how it is represented within the brain. However, relatively few contributions deal with the physical mechanism underlying the compass, the principal subject of this paper. Only one attempt has been made (to our knowledge) to design a navigational aid for a drone or robot based on this compass; this uses only 3 pairs of photoreceptors (Wehner,1997; Lambrinos et al, 1998), different from the typical fan of 50 -100 pairs of receptors

J. Smith F. (2008).
A NEW ALGORITHM FOR NAVIGATION BY SKYLIGHT BASED ON INSECT VISION.
In *Proceedings of the First International Conference on Bio-inspired Systems and Signal Processing*, pages 185-190
DOI: 10.5220/0001068901850190
Copyright © SciTePress

used by an insect or used in the design proposed here. NASA has also built robots navigating by skylight, but these use three photoreceptors with different axes of polarization, probably the underlying principle behind navigation by the ocelli (NASA, 2005). Few details have been released on the above systems, so comparison with our new algorithm has not been possible.

In the following we first derive mathematical expressions for the light intensities measured by the photoreceptors, before showing how these can give the direction of the sun.

2 THEORY

2.1 Measured Intensity

We begin with the assumption that the sky is blue, with no cloud. Then it is well known (Rayleigh, 1871) that the light observed from any patch of sky is partially polarised, with an elliptical profile for the electric vector (although not elliptically polarised) in which the major axis of the ellipse, is at right angles to both the direction of the sun, represented by the unit vector **S,** and to the direction of the observed patch of sky, **k'**. We let **k'** be one of three mutually orthogonal vectors **i', j'** and **k'**, with **i'** in the direction of the major axis of the ellipse, and **j'** in the direction of the minor axis. The electric vector in the direction of the major axis is often called the E-vector. The angle which this makes clockwise in the ellipse from the plane of the zenith, is called the polarization angle, χ. In the ideal situation where all of the light observed is scattered once only, the ratio of the size of the minor axis to the size of the major axis is known to be cos *(θ)* where θ is the angle between **S** and **k'**.

Let $\mathbf{E_S}$ be the scattered electrical vector being observed. Then

$$\mathbf{E_S} = E[\cos(\phi)\,\mathbf{i'} + \cos(\theta)\sin(\phi)\mathbf{j'}] \qquad (1)$$

where E is the magnitude of the unpolarized electric field. The angle ϕ determines the direction of the vector within the ellipse; so it equals 0 when the electric vector is parallel to the major axis.

When the partially polarised light enters an ommatidium in the dorsal rim its intensity is measured by two photoreceptors, each of which can measure polarised light with parallel structures called microvilli. The two directions of the microvilli are at right angles to one another, and define two orthogonal axes of polarization, represented here by the orthogonal unit vectors **i** and **j**, known as the X and Y photoreceptors. The third mutually orthogonal vector, **k**, is in the same direction as the observed patch of sky, so **k** = **k'**. The angle which the vector **i** makes with the vertical plane by rotation about **k** is called ξ.

We can now write the previous unit vectors in Equation (1) in terms of **i** and **j** using the transformation:

$$\begin{aligned} \mathbf{i'} &= +\cos(\chi-\xi)\mathbf{i} + \sin(\chi-\xi)\mathbf{j} \\ \mathbf{j'} &= -\sin(\chi-\xi)\mathbf{i} + \cos(\chi-\xi)\mathbf{j} \end{aligned} \qquad (2)$$

We look at the orientations of the microvilli in the dorsal rim of the honey bee by Sommer (1979), as copied in Figure 1. The fan shape of the microvilli is apparent.

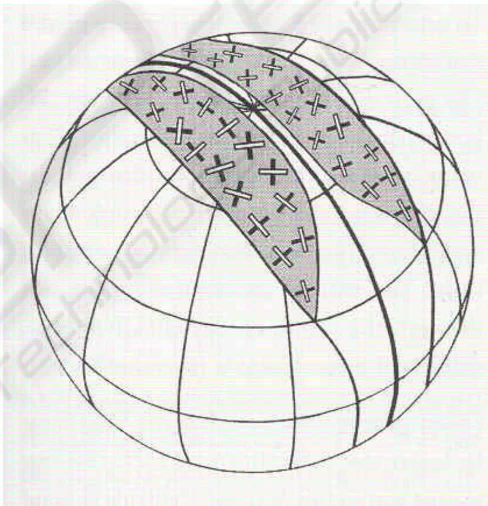

Figure 1: The paired orthogonal photoreceptors in the dorsal rims of a bee. The Y photoreceptors are dark, the X photoreceptors light (Sommer, 1979).

The observation of sky by the photoreceptors is known to be contralateral, i.e. they observe the sky on the opposite side of the head. An examination of the figure shows that the axes of the X photoreceptors are approximately parallel to the meridians passing through the patches of sky being observed contralaterally. The same approximate parallel pattern was found in Desert Ants by Wehner and Raber (1979). So we assume that the angle ξ that the X polarization axis makes with this meridian is always zero. This greatly simplifies our later algorithm for a small insect brain.

We can now substitute for **i**' and **j**' from Eq.(2) in Eq.(1) to obtain an expression for the partially polarised vector $\mathbf{E_S}$ in terms of the unit vectors **i** and

j. For example, part of this is the magnitude, E_X, of the vector in the direction **i** to be measured by the microvilli of the X photoreceptor:

$$E_X = E\left(\cos(\chi)\cos(\phi) - \sin(\chi)\cos(\theta)\sin(\phi)\right) \qquad (3)$$

However, each receptor can only measure a light intensity, which is proportional to the summation of the square of the amplitudes of the electrical vectors for all angles ϕ. So, for receptor X, the measured intensity, S_X, is found by first integrating the square of the amplitude in (3) over all angles and then multiplying by a factor, $2R$, which depends on terms derived by Lord Rayleigh (1871) and on the measuring capability of the photoreceptor.

Before writing down the result of the integration we note that in the real world the sky is often not always blue, but has a degree of haze or cloud differing with direction. The light then entering the ommatidia can be viewed as make up of two components, one partly polarised as in the above equations, and the second totally unpolarized due to multiple scattering. We let U be the intensity of unpolarized light measured by both photoreceptors. Then we find

$$S_X = RE^2\left[1 - \sin^2(\theta)\sin^2(\chi)\right] + U \qquad (4)$$

$$S_Y = RE^2\left[1 - \sin^2(\theta)\cos^2(\chi)\right] + U \qquad (5)$$

It has been shown by Labhart(1988) that the POL neuron at the bottom of each ommatidium of a cricket records the difference between the two signals, or rather the difference between the log of the two signals, not the signals themselves; so the signal recorded is

$$S_{XY} = Ln(S_X) - Ln(S_Y) \qquad (6)$$

We set $RE^2 = 1$ in Figure (2) to illustrate the variation in these signals as the azimuth angles of the ommatidia vary.

Some of the above is known, but to proceed further we need the polarization angle, χ. This depends on the azimuth and elevation of the sun.

2.2 Solar Azimuth and Elevation

The angles θ and χ are related to the azimuth, a_s, and elevation, h_s, of the sun. It is convenient to introduce a third set of orthogonal axes, **i'', j''** and **k''** fixed on the earth, with **i''** and **j''** in the plane of the ground and **k''** vertically upwards. For a photoreceptor to find θ and χ we need also the azimuth, a_o, and elevation, h_o, of the sky being observed by the photoreceptor, i.e. towards the centre of the patch of sky being observed. So we let the unit vector **i''** point along the ground in this direction.

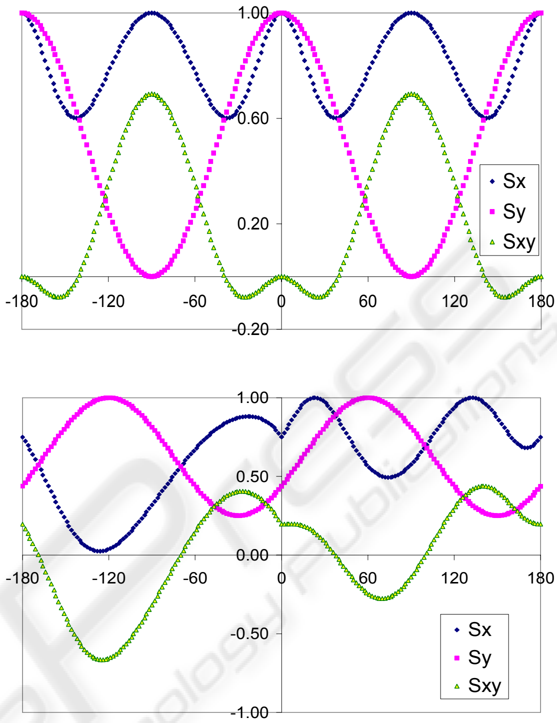

Figure 2: Illustration of the signals S_X and S_Y with U=0, and S_{XY} with U=1, as they vary with the azimuth of the fan of observations, a_o, measured from the central axis of the insect. Top graph: h_s=0, a_s=0. Bottom: h_s=30, a_s=60. Note that a_s=a_o at a maximum of S_Y and that there are 4 azimuths where S_{XY}=0, called zeros.

In terms of these new unit vectors we write the vector pointing in the direction of the sun as **S** = S_1**i''** + S_2**j''** + S_3**k''** where

$$S_1 = \cos(h_s)\cos(a_s - a_o);$$
$$S_2 = \cos(h_s)\sin(a_s - a_o); \qquad (7)$$
$$S_3 = \sin(h_s)$$

We can write down two equations for the direction of the sun. First we know that the vector **k'**, which points at the observed patch of sky, makes an angle θ relative to the direction of the sun, **S**. We also know that the E-vector, in the direction represented by the unit vector, **i'**, is at right angles to the plane containing the solar unit vector, **S**, and the vector, **k'**. So

(a) **k'.S** = $cos(\theta)$, and (b) **i'.S** = 0. (8)

We now express the unit vectors **i'**, describing the E-vector, and **k'** in terms of the new axes **i'', j''** and **k''** fixed in the earth. Since **k'** and **k''** are in the same vertical plane it follows that

$$\mathbf{k}' = \cos(h_o)\mathbf{i}'' + \sin(h_o)\mathbf{k}'' \quad (9)$$

Noting that **i'** is at right angles to **k'** and that the angle χ represents the orientation of the major axis of the polarised light about the vector **k'**, it follows that

$$\mathbf{i}' = [-\sin(h_O)\mathbf{i}'' + \cos(h_O)\mathbf{k}'']\cos(\chi) - \sin(\chi)\mathbf{j}'' \quad (10)$$

Substitute and Equations (8a and b) become

$$\cos(\theta) = \cos(h_O)\cos(a)\cos(h_S) + \sin(h_O)\sin(h_S) \quad (11)$$

$$0 = \cos(\chi)\cos(h_O)\sin(h_S)$$
$$-\cos(\chi)\sin(h_O)\cos(a)\cos(h_S) - \sin(\chi)\sin(a)\cos(h_S) \quad (12)$$

where $a = a_s - a_o$ is the azimuth of the sun relative to the azimuth of the observed sky.

A new unexpected equation was derived from (11) and (12) after some analysis:

$$\sin(\theta)\cos(\chi) = \sin(a_s - a_o)\cos(h_s) \quad (13)$$

This can also be derived geometrically, or from the relation **k'** x **S** = *sin(θ)***i'.** It simplifies the calculation of the angle χ, although not its sign. But more significantly, by substitution in (5), it changes the expression for the measured intensity S_Y:

$$S_Y = RE^2\left[1 - \sin^2(a_s - a_o)\cos^2(h_s)\right] \quad (14)$$

This surprising result shows first that it is the same for all elevations of the sky being observed and second that, as the azimuth a_o round the fan of receptors varies, the position of the maximum value of S_Y gives a new measure for the azimuth of the sun, for all elevations of the sun (see Figure 2). Unfortunately, finding this maximum is not possible if an insect is only measuring the difference in the two log signals as in Equation (5). But this does not stop a robot from using this strategy to find the solar azimuth. But it can only be approximate as finding the exact position of a maximum is always difficult.

2.3 A Precise Compass

We begin with a question - why have two orthogonal photoreceptors, instead of one? A possibility is that the contrast between the two signals is improved near the maximum of one of them. Unfortunately this is often obscured by the s*in²(θ)* term in Equations (4) and (5), as evident in Figure (2). Also we are left with the problem of the lack of precision in the determination of the position of any maximum, even enhanced.

The photoreceptors can only measure intensities, but absolute intensities of light from the sky are so variable that only comparisons between intensities from the same region of the sky are meaningful computationally. An example is the ratio of the two intensities from the pair of orthogonal receptors in one ommatidium. Although this ratio can be measured accurately, the inclusion of an unknown amount of unpolarized light, *U*, makes it meaningful only when the two are equal (the easiest factor to measure). Equating S_X and S_Y puts $S_{XY} = 0$ in Equation (6), eliminates *U, RE²* and θ and we get simply: $\sin^2(\chi) = \cos^2(\chi)$.

This makes χ = ±π/4. So finding where S_{XY}=0, the quantity measured for each ommatidium, tells us the precise azimuths a_o where χ = ±π/4. We call this a zero. An examination of Figure (2) shows that in these two cases there are 4 zeros. Curves similar to this were drawn for a range of solar azimuths and solar elevations and the zeros found. The zeros for different solar azimuths are shown in Figure (3) for one solar elevation. This and other examples show that in almost all cases there are 4 zeros, usually 2 on either side of the head, but sometimes 4 on one side and none on the other. When the elevation of the sun is above the elevation of the observed patch of sky there may be no zeros.

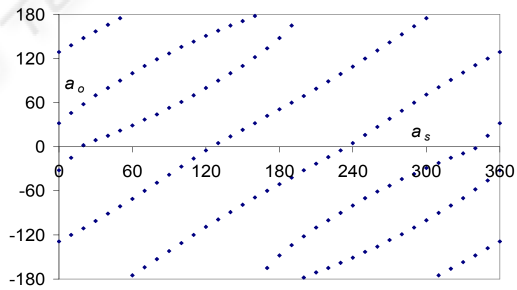

Figure 3: Graph of azimuths, a_o, of the observation at which S_{xy} = 0 (called zeros) for different values of the solar azimuth, a_s, at solar elevation, h_s =30°. Zeros occur when the two orthogonally polarized intensities are equal, making *χ=±π/4*. There are usually 4 zeros, just enough to uniquely define the azimuth and elevation of the sun.

We now show how we can use these 4 zero to make a precise measurement of the sun's position. Noting that cos(χ) = 1 and sin(χ) = ±1 at the zeros, Equation (12) becomes:

$$\cos(a_s - a_o)\sin(h_o)$$
$$\pm\sin(a_s - a_o) = \cos(h_o)\tan(h_s) \quad (15)$$

Solving this for a_s, the azimuth of the sun, gives

$$a_s = a_o \pm \gamma \pm \delta \qquad (16)$$

in which for each azimuth, a_o there is a different γ and δ given by $\gamma = arccos(1/K)$ and $\delta = arcsin(tan(h_s)cos(h_o)/K)$ where $K^2 = 1+ sin^2(h_o)$. The angle γ is fixed for each ommatidium; so it might be stored as $a_o \pm \gamma$ within the corresponding neurons. It needs to be corrected with the angle δ (unless the sun is on the horizon, when $\delta=0$); but this correction needs the observation of 4 zeros, as discussed in the next section. If 4 zeros cannot be observed because the region of observed sky is restricted the insect can only use $a_o \pm \gamma$, leaving an error of δ. Such errors have been found in experiments. So Equation (16) may be the mathematical basis of at least part of the celestial map in an insect brain.

The 4 alternatives in Equation (16) can also regenerate exactly the results in Figure (3), but in an inverted form. An example is shown in Figure (4). In Figures (3) and (4) the elevations of the sky being observed have been chosen to vary between 45° (at azimuths 0° and 180°) and 80° (at azimuths ±90°). However, these elevations are not critical: if all ommatidia examine the sky at a constant high elevation the algorithm described below is still valid and the curves in Figures (3) and (4) all become straight lines. There are still 4 zeroes, but none at high solar elevations where $sin(\delta) > 1$.

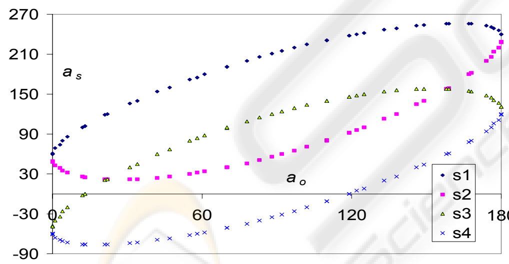

Figure 4: Inverted graph of a_s for positive a_o calculated using Equation (16) for h_s =60°, showing the contribution of the different ± combinations: s1: a_o +γ +δ; s2: a_o +γ -δ; s3: a_o –γ +δ; s4: a_o –γ -δ.

We have built a simulator that can calculate the position of the sun using the above equations. We illustrate first with an example in which the elevation of the sun is 30° and the solar azimuth is 20 °; in this example the four zeros are at the azimuths: a_o = 53°, 145 °, -5 °, and -110 °. For each of these there are 4 alternatives given by Equation (16), but an insect or a robot which is only measuring intensities would not know which is correct. Four alternatives for 4 zero angles makes a total of 16 possibilities as in the array in Table 1.

Table 1: Example of array of 4 possible solar azimuths for each of 4 zeros (where S_X - S_Y = 0) when the elevation of the sun is 30°. Note that the correct azimuth (marked in bold) is found once in each of the four rows corresponding to the four zeros. This occurs only for the correct solar elevation.

Zeros	γ+δ	+γ-δ	−γ+δ	−γ-δ
52	180	**20**	85	-75
145	-89	125	165	**20**
-5	131	**20**	-31	-142
-110	**20**	-148	-72	120

So the algorithm is simple:

1. find the 4 zeros where $S_X = S_Y$;
2. obtain for each the two angles $a_o \pm \gamma$;
3. choose a possible solar elevation;
4. find the 4 possible azimuths for each zero from Equation (16) and put in an array of 16 angles (as in the example);
5. scan the array for one angle in all 4 rows, within a small tolerance (e.g. 1 degree). If found, it is the solar azimuth;
6. if not found, increase the elevation (e.g. by 1 degree) and return to step 3.

Figure (5) shows how this algorithm converges to the correct result for the example in Table 1.

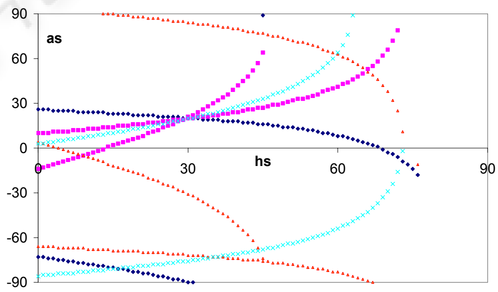

Figure 5: Graph showing, as the solar elevation h_s varies, how four of the elements in the 16 array elements in Table 1 converge on the correct result at the solar azimuth a_s=20° when h_s=30°. (Only half of the graph is shown.).

Simulations with about 1000 examples have shown that this algorithm succeeds is almost every case with no ambiguity within a tolerance of 1 degrees. Occasional errors or failure occur only at low or high solar elevations (< 3° or > h_o). Four zeros are needed: three zeros give a typical 40% error rate. The algorithm takes only a page of code, and once it is given the positions of the 4 zeros it calculates the solar azimuth in less than a second on a PC. It can easily be built into the processor of any robot.

Besides the accuracy of the method it has the advantage that it gives the solar azimuth anywhere within 360^{o}, with no ambiguity of π as in some other algorithms. It is partially independent of environmental conditions since some ommatidia may be looking at blue sky while others are looking at lightly clouded sky. The position of the zeros is unchanged as long as a polarization pattern is detectable below the cloud, which is more likely for ultraviolet light detectors (Pomozi et al., 2001).

So the greatest difficulty in building a skylight compass for a robot based on this algorithm is the detection of the four zeros. One design uses an array of about 100 pairs of orthogonal photoreceptors in a circle round the robot. The problem is that each pair would have to observe a patch of sky with an accurate azimuth; the elevation, due to Equation (14), would be less critical. In another design the robot has one accurate pair of photoreceptors which is rotated continually through 360^{o} (like radar) measuring the azimuth as it moves at a constant high elevation (e.g. 70^{o}).

3 CONCLUSIONS

We have shown that an accurate celestial compass for a robot can be built round the principle of finding 4 zeros in the differences between the two signals obtained from pairs of orthogonally polarised photoreceptors. The algorithm was derived from published studies on the anatomy of insect eyes and on published experiments with insect navigation. In particular Equation (16) explains why errors occur when the view of an insect is restricted. The algorithm is also simple enough for the small brain of an insect; so we believe that the algorithm, or something like it, is part of the celestial compass within the brain of an insect.

At the heart of the algorithm are searches in arrays of exactly 16 elements as in Table 1. So we might expect evidence for this within the brain of an insect. It is interesting to note that a topographic representation of E-vector orientation has been found to underlie the columnar organisation of the central complex of the brain of a locust, and this consists of stacks of arrays, each composed of a linear arrangement of 16 columns (Heinze and Homberg, 2007).

REFERENCES

Bernard, G D, Wehner, R, 1977. Functional similarities between polarization vision and color vision, Vision Res., 17, 1019-28.

Fent, K, Wehner, R, 1985. Ocelli: A celestial compass in the desert ant Cataglyphis, Science, 228, 192-4.

Goodman, L. J., 1970. The structure and function of the insect dorsal ocellus. Adv. Insect Phys., 7, 97-195.

Heinze, S, Homberg, U, 2007. Maplike Representation of Celestial E-Vector Orientations in the Brain of an Insect, Science, 315, 995-7.

Kirschfeld, K, Lindauer, M, Martin,H, 1975. Problems in menotactic orientation according to the polarized light of the sky, Z. Naturforsch, 30C, 88-90.

Labhart, T, 1980. Specialized Photoreceptors at the dorsal rim of the honeybee's compound eye: Polarizational and Angular Sensitivity, J Comp. Phys., 141, 19-30.

Labhart, T, 1988. Polarised-opponent interneurons in the insect visual system, Nature, 331, 435-7.

Lambrinos, D, Maris, M, Kobayashi, H, Labhart, T, Pfeifer, P, Wehner, R, 1998. Navigation with a polarized light compass, Self-Learning Robots II: Bio-Robotics (Digest 1998/248) IEE, London, 7/1-4.

NASA, 2005. www.nasatech.com/Briefs/Oct05/ NPO_41269.html

Pomozi, I, Horvath, G, Wehner, R., 2001. How the clear-sky angle of polarization pattern continues underneath clouds, J. Expt. Biol, 204, 2933-42.

Rayleigh, Lord, 1871. On the light from the sky, its polarisation and colour, Phil Mag,, 41, 107-20, 274-9.

Rossel, S, 1993. Mini Review: Navigation by bees using polarised skylight, Comp. Biochem. Physiol, 104A, 695-705.

Rossel, S, and Wehner, R, 1982. The bee's map of the e-vector pattern in the sky, Proc. Natl. Acad. Sci. USA, 79, 4451-5.

Sommer, E W, 1979. Untersuchungen zur topographischen Anatomie der Retina und zur Sehfeldoptologie im Auge der Honigbiene, Apis mellifera (Hymenoptera). PhD Thesis,Un.Zurich.

Tyndall, J, 1869. On the blue colour of the sky, the polarisation of skylight, and on the polarisation of cloudy matter, Proc. Roy. Soc., 17, 223.

Von Frisch, K, 1949. Die Polarisation des Himmelslichts als Orientierender Faktor bei den Tanzen der Bienen, Experientia, 5, 142-8.

Wehner, R, 1989. The hymenopteran skylight compass: matched filtering and parallel coding, J Exp. Biol., 146, 63-85.

Wehner, R, 1997. The Ant's celestial compass system: spectral and polarization channels, In Orientation and Communication in Arthropods, Ed. M. Lehler, Birkhauser, Berlag, Basel, Switzerland, 145-85.

Wehner, R, and Raber, F, 1979. Visual spatial memory in desert ants, Cataglyphis bicolor (Hymenoptera: Formicidae), Experientia, 35, 1569-71.